Two-stage Approach for the Provision of Time-Dependent Flexibility at TSO-DSO Interface

Georgios C. Kryonidis
School of Electr. & Comput. Eng.
Aristotle University of Thessaloniki
Thessaloniki, Greece
kryonidi@ece.auth.gr

Apostolos N. Lois
School of Electr. & Comput. Eng.
Aristotle University of Thessaloniki
Thessaloniki, Greece
aposlois@ece.auth.gr

Kyriaki-Nefeli D. Malamaki
School of Electr. & Comput. Eng.
Aristotle University of Thessaloniki
Thessaloniki, Greece
kyriaki_nefeli@hotmail.com

Charis S. Demoulias
School of Electr. & Comput. Eng.
Aristotle University of Thessaloniki
Thessaloniki, Greece
chdimoul@auth.gr

2021 International Conference on Smart Energy Systems and Technologies (SEST) | 978-1-7281-7660-4/21/$31.00 ©2021 IEEE | DOI: 10.1109/SEST50973.2021.9543347

***Abstract*—In this paper, a new methodology is presented for the provision of active and reactive power flexibility at the transmission and distribution system operator (TSO-DSO) interface. Its distinct feature is the effective integration of time-dependent flexibility resources, e.g., energy storage systems, thus moving a step closer to the accurate modeling of active distribution grids. The proposed methodology is part of the day-ahead analysis and is divided into two main stages. In the first stage, an iterative, optimization-based process is adopted to estimate the hourly flexibility areas at the TSO-DSO interface that maximize the daily flexibility capacity of the distribution grid. These areas can be used in the day-ahead scheduling of the electrical grid to determine the optimal power set-points at the TSO-DSO boundary nodes. The second stage is introduced to optimally coordinate the operation of the main network elements to meet the above set-points. The validity of the proposed methodology is demonstrated by performing simulations on a medium-voltage grid with radial configuration.**

***Index Terms*—Distributed generation, energy storage systems, flexibility, optimization, TSO-DSO interface.**

I. Introduction

A. Background

Driven by the proliferation of small-scale renewable energy sources (RESs), distribution networks have faced a transition from passive to active operation, bringing a new era to the electrical grid. Nevertheless, this era is characterized by high levels of uncertainty due to the stochastic and intermittent nature of RESs that may jeopardize the secure and reliable grid operation [1]. A promising solution to this issue is the provision of flexibility services from distribution grids to the transmission system [2]. By adopting this approach, the apparent power exchanged with the transmission system can be adjusted to compensate the impact of generation uncertainty on the grid performance.

B. Relevant Literature

It is evident that the accurate estimation of the flexibility that can be provided from the distribution grids is an important step towards the realization of this solution. In the literature, several methodologies have been developed to estimate the flexibility at the transmission and distribution system operator (TSO-DSO) interface. More specifically, the authors in [3] propose a two-stage approach to optimally aggregate and disaggregate the flexibility provided from the distributed energy resources. Furthermore, in [4], an accurate model of consumers's behavior is considered to estimate the aggregated flexibility at the TSO level. However, both approaches assume that the flexibility resources (FRs) are fully exploitable, neglecting possible limitations that may occur due to the violation of technical constraints in distribution grids. To overcome this, power flow analysis is used in [5] to determine the feasible flexibility operating points at TSO-DSO interface. An improved version of [5] is proposed in [6] by introducing a probabilistic analysis to deal with generation and consumption uncertainty. Nevertheless, these solutions are characterized by a prohibitive computation burden, since numerous power flow calculations should be performed to evaluate the feasibility of all the possible combinations of the FRs operating points.

An alternative approach is presented in [7], where the flexibility area is calculated by solving an iterative, optimization-based algorithm. More specifically, at each iteration an optimal power flow (OPF) problem is solved, taking into account the nonlinear behavior and the technical constraints of the distribution grid. Based on the acquired results, the OPF parameters are updated and a new OPF problem is solved at the next iteration, until convergence is achieved. Similar solutions are proposed in [8] and [9] that slightly differentiate on the update process of the OPF parameters. Moreover, enhanced versions of [7]–[9] are proposed in [10] and [11], where the on-load tap changer (OLTC) of the high-/medium-voltage (HV/MV) transformer is introduced in the OPF formulation as an additional control variable. Furthermore, to reduce the computational complexity of the OPF problem, linearized versions of the initial OPF formulation are adopted in [12]–[14]. However, linearized-based approaches introduce inaccuracies and may lead to infeasible operating conditions. Finally, the authors in

978-1-7281-7660-4/21/$31.00 ©2021 IEEE

[15] propose a hybrid approach consisting of two stages. In the first stage, a linearized OPF problem is solved to estimate the flexibility area. The estimated values are then used as inputs in the second stage, where the conventional, nonlinear OPF problem is solved to derive the final flexibility area.

As a common drawback, all the above-mentioned methods present a limited applicability since they calculate the flexibility area for a specific time instant. In case multiple time instants are considered, the impact of time-dependent FRs (TDFRs), e.g., energy storage systems (ESSs), on the flexibility areas is ignored. As a result, overestimated flexibility areas may occur since the operating state of TDFRs of the previous/next time instants is neglected, leading also to infeasible operating points at the TSO-DSO interface. An attempt to solve this problem is proposed in [16], where a fixed operation pattern is considered for the TDFRs. In this way, the problem is simplified to calculating the flexibility areas for each time instant separately. However, the impact of the operation pattern on the flexibility area is not examined.

C. Main Contributions

In this paper, a new methodology is presented for flexibility provision at the TSO-DSO interface, which is suitable for the day-ahead planning of the electrical grid. The main contributions are listed below:

- *Ability to handle TDFRs*: Contrary to current solutions proposed in the literature, the proposed methodology can effectively integrate TDFRs in the flexibility provision, thus allowing a more accurate representation of distribution grids.
- *Introduction of the concept of hourly (HFA) and daily flexibility areas (DFA)*: To facilitate the integration of TDFRs in the proposed methodology, two types of flexibility areas are proposed, namely HFA and DFA.
- *Two-stage approach*: The proposed methodology consists of two stages. In the first stage, an iterative, optimization-based process is employed to determine the HFAs at the TSO-DSO interface that maximize the DFA of the distribution grid. The second stage is applied to optimally dispatch the FRs to meet the operating set-points at the TSO-DSO interface.

II. Proposed Methodology

A. Overview

The main outline of the proposed methodology is presented in Fig. 1 consisting of two distinct stages. Scope of the first stage is to estimate the HFAs. HFA is calculated using hourly data and is defined as the region in the PQ plane that includes all the feasible combinations of active (P^t_{TD}) and reactive power (Q^t_{TD}) at the TSO-DSO interface for a given hour t. Since hourly data are employed, the terms energy and power are used interchangeably. In this paper, the HFA is measured is terms of energy, i.e., in VAh[2], to be in line with the physical meaning of the HFA.

A strong interdependency among the estimated flexibility areas exists due to the use of TDFRs where the operating state for a given hour is coupled with the operating state of previous/next hours. To include this interdependency in the HFA estimation, a multi-period optimization algorithm is introduced. The proposed algorithm targets at the maximization of the DFA at the TSO-DSO interface. DFA is defined as the region that includes all the feasible combinations of daily active ($\sum_{t\in T} P^t_{\mathrm{TD}}$) and reactive energy ($\sum_{t\in T} Q^t_{\mathrm{TD}}$) at the TSO-DSO interface. Here, T is the time horizon set, i.e., one day. This process can be performed by the DSO or an Aggregator which acts as a representative in the energy market.

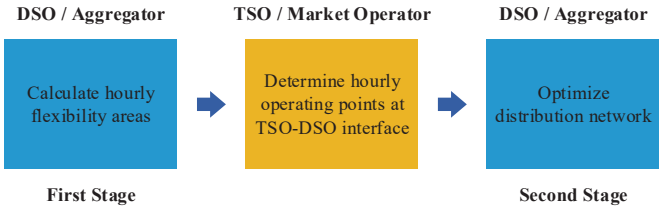

Fig. 1. Overview of the two-stage methodology.

The estimated HFAs in conjunction with the corresponding costs are used by the TSO or the Market Operator for the day-ahead planning of the electrical grid. It is worth mentioning that the derivation of the relevant costs is considered out of the scope of this paper. The outcomes of the day-ahead planning are the active and reactive power operating points at the TSO-DSO interface for each hour. To meet these power set-points, the second stage of the proposed methodology is activated, where a multi-period optimization algorithm is applied to optimally coordinate the FRs of the distribution grid.

In the next subsections, the mathematical formulation of the proposed two-stage methodology is analytically presented.

B. First Stage

The mathematical formulation of the multi-period optimization algorithm comprises the following: (a) objective function, (b) equality, and (c) inequality constraints. The equality constraints are employed to model the distribution grid, while inequalities pose the corresponding operating limits. Moreover, two FR types are considered which are introduced as control variables to the optimization problem, namely the reactive power of distributed generation (DG) units and the active power of ESSs. Note that additional FR types can be used as control variables without affecting the process for the derivation of the maximum DFA.

The objective function is formulated as follows:

$$\min_{Q^t_{\mathrm{g},i},P^t_{\mathrm{b},i}} \left(\alpha \sum_{t\in T} P^t_{\mathrm{TD}} + \beta \sum_{t\in T} Q^t_{\mathrm{TD}} \right) \tag{1}$$

where $Q^t_{\mathrm{g},i}$ and $P^t_{\mathrm{b},i}$ are the control variables denoting the reactive power of the DG unit and the active power of the ESS, respectively, connected to node i during hour t. α and β are two weight coefficients. Furthermore, P^t_{TD} and Q^t_{TD} can be calculated by:

$$P^t_{\mathrm{TD}} = \sum_{j\in N} P^t_{sj} \tag{2}$$

$$Q^t_{\mathrm{TD}} = \sum_{j\in N} Q^t_{sj} \tag{3}$$

where N stands for the set of network nodes. Moreover, P_{sj}^t and Q_{sj}^t are the active and reactive power flowing from slack bus (s) to the directly connected node j. Generally, the power flows between two directly connected network nodes, e.g., i and j, are calculated according to (4) and (5).

$$P_{ij}^t = V_i^t V_j^t [G_{ij} \cos(\theta_i^t - \theta_j^t) + B_{ij} \sin(\theta_i^t - \theta_j^t)] \quad (4)$$

$$Q_{ij}^t = V_i^t V_j^t [G_{ij} \sin(\theta_i^t - \theta_j^t) - B_{ij} \cos(\theta_i^t - \theta_j^t)] \quad (5)$$

Here, V_i^t and θ_i^t stand for the magnitude and angle of the voltage at node i during hour t, whereas G_{ij} and B_{ij} are the real and imaginary part of the ij-th element of the network admittance matrix. Regarding slack bus, a zero voltage angle is assumed, while the voltage magnitude at hour t (V_s^t) is calculated according to (6) to model the OLTC operation.

$$V_s^t = V_{\text{hv}}^t / [m(1 + tap^t \delta / 100)] \quad (6)$$

V_{hv}^t and tap^t are the voltage magnitude of the HV network and tap position at hour t, δ stands for the variation of the transformation ratio per tap position change, and m is the nominal voltage transformation ratio. Moreover, the active (P_i^t) and reactive power (Q_i^t) injections are calculated by:

$$P_i^t = \sum_{j \in N} P_{ij}^t = P_{\text{g},i}^t + P_{\text{b},i}^t - P_{\text{c},i}^t \quad (7)$$

$$Q_i^t = \sum_{j \in N} Q_{ij}^t = Q_{\text{g},i}^t - Q_{\text{c},i}^t \quad (8)$$

where $P_{\text{g},i}^t$ is the output active power of the DG unit, while $P_{\text{c},i}^t$ and $Q_{\text{c},i}^t$ are the active and reactive power of the load, respectively. Eqs. (9) and (10) are introduced to model the ESS.

$$SoC_i^{t+1} = SoC_i^t - s_i^t \frac{P_{\text{b},i}^t}{\eta_i E_{\text{b},i}} - (1 - s_i^t) \frac{\eta_i P_{\text{b},i}^t}{E_{\text{b},i}} \quad (9)$$

$$P_{\text{b},i}^t (s_i^t - 0.5) \geq 0 \quad (10)$$

Here, SoC_i^t is the state of charge of the ESS connected to node i during hour t, whereas $E_{\text{b},i}$ and η_i are the corresponding nominal capacity and charging/discharging efficiency, respectively. s_i^t is an auxiliary binary variable used to differentiate the charging from the discharging process in the calculation of the state of charge. The operating constraints of the ESSs are presented below:

$$SoC_{\min,i} \leq SoC_i^t \leq SoC_{\max,i} \quad (11)$$

$$-P_{\max,i} \leq P_{\text{b},i}^t \leq P_{\max,i} \quad (12)$$

where $P_{\max,i}$, $SoC_{\min,i}$, and $SoC_{\max,i}$ are the permissible limits of the ESS. Eq. (13) is used to model the reactive power capability of the DG units, where $S_{\text{g},i}$ is the nominal apparent power of the DG unit connected to node i.

$$-\sqrt{{S_{\text{g},i}}^2 - {P_{\text{g},i}^t}^2} \leq Q_{\text{g},i}^t \leq \sqrt{{S_{\text{g},i}}^2 - {P_{\text{g},i}^t}^2} \quad (13)$$

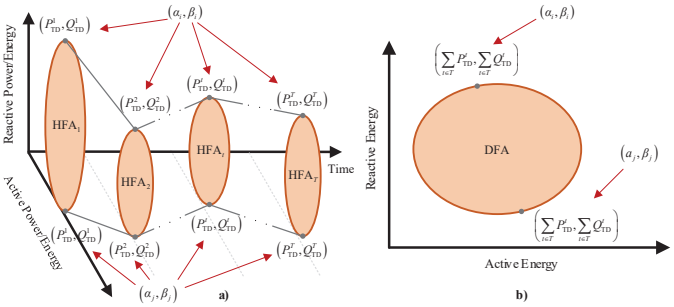

Fig. 2. Graphical representation of HFAs and DFA.

Finally, (14) and (15) are introduced to model the technical constraints of the distribution grid.

$$V_{\min} \leq V_i^t \leq V_{\max} \quad (14)$$

$$\sqrt{{P_{ij}^t}^2 + {Q_{ij}^t}^2} \leq S_{\max,ij} \quad (15)$$

$V_{\min}$ and $V_{\max}$ are the minimum and maximum voltage limits, respectively, while $S_{\max,ij}$ is the maximum apparent power flowing through the line connecting nodes i and j.

The DFA is constructed following the iterative process proposed in [7]. Specifically, at each iteration, the multi-period optimization problem of (1)-(15) is solved assuming a different set of the weight coefficients α and β. The resulted daily operating point lies in the perimeter of the DFA. The final estimated DFA is constructed by combining all the daily operating points. A graphical representation of this iterative process is presented in Fig. 2. Note that the accuracy of the estimated DFA is increased with the number of the iterations.

C. Second Stage

The second stage is employed to optimally coordinate the FRs to meet the active and reactive power profiles at the TSO-DSO interface determined in the day-ahead planning. This is attained by solving a new multi-period optimization problem where the main objective is to improve the ESSs lifetime by minimizing their usage. The corresponding objective function is mathematically described in (16).

$$\min_{Q_{\text{g},i}^t, P_{\text{b},i}^t} \sum_{t \in T} |P_{\text{b},i}^t| \quad (16)$$

To reduce the computational complexity posed by the absolute value operator, (16) is modified as follows:

$$\min_{Q_{\text{g},i}^t, P_{\text{b},i}^t} \sum_{t \in T} P_{\text{b},i}^{\text{abs},t} \quad (17)$$

$$P_{\text{b},i}^t = P_{\text{b},i}^{+,t} - P_{\text{b},i}^{-,t} \quad (18)$$

$$P_{\text{b},i}^{\text{abs},t} = P_{\text{b},i}^{+,t} + P_{\text{b},i}^{-,t} \quad (19)$$

where $P_{\text{b},i}^{\text{abs},t}$ is the absolute value of $P_{\text{b},i}^t$ calculated according to (18) and (19) using two auxiliary non-negative variables, namely $P_{\text{b},i}^{+,t}$ and $P_{\text{b},i}^{-,t}$. The reason behind the use of these auxiliary variables lies in the following rationale: Every real number x_{real} can be mathematically expressed as the difference of two non-negative numbers, i.e., $x_+ - x_-$. Among the

infinite combinations, the absolute value x_{abs} corresponds to the pair of the non-negative numbers that minimizes the sum $x_+ + x_-$. Thus, due to the use of (17) as a minimization objective, the pair of the non-negative numbers and thus the absolute value are correctly calculated [17]. Finally, the equality and inequality constraints as expressed by (2)-(15) are also used in the second stage. The main difference is that P^t_{TD} and Q^t_{TD} are replaced by $P^t_{\mathrm{TD,set,}}$ and $Q^t_{\mathrm{TD,set}}$, respectively, which are derived from the day-ahead analysis.

III. Numerical Results

The performance of the proposed two-stage methodology is assessed on the day-ahead planning of the 20 kV MV distribution grid depicted in Fig. 3. Details regarding the network characteristics, the location and the rated power of loads and photovoltaic (PV) units, which are the only DG type considered in the simulations, are presented in [18]. Furthermore, to model TDFRs, three ESSs are added to nodes 4, 20, and 30 of the examined grid. The ESSs are identical and their technical characteristics are presented in Table I.

The two stages of the proposed methodology are evaluated in the next subsections. Considering the network parameters, V^t_{hv} and tap^t are kept constant and equal to 1 pu, and -4, respectively. Moreover, the ESSs are assumed fully charged at the beginning of the day, while the hourly generation and consumption profiles used in the simulations are derived from the dataset presented in [19]. Finally, all the examined scenarios are solved in GAMS using the BONMIN solver [20].

A. Evaluation of the First Stage

The first stage of the proposed methodology is compared against the following solutions presented in the literature:

- Conventional solution [7]–[11]. In this approach, the time-dependency of ESSs is ignored allowing any exchange of active power with the grid lying between the limits posed by (12). This is a simplified version of the multi-period optimization problem of (1)-(15) by removing (9)-(11).
- Fixed TDFR operation pattern [16]. In this case, the ESSs output power follows a predefined profile respecting (9)-(12). The ESSs power profile is defined *a priory* using the day-ahead generation and consumption forecasts. Here, ESSs are assumed to operate in a peak shaving mode.

Assuming a single-day analysis, the HFAs and the DFAs at the TSO-DSO interface are presented in Figs. 4 and 5, respectively, for all the examined methods. Furthermore, the derived DFAs are quantified and compared in Table II. Note that the proposed methodology is used as the reference case for the comparisons. Finally, the projections of the HFAs, which are derived from the first stage of the proposed method, on the active power and reactive power axes are depicted in Fig. 6.

According to Figs. 4-5 and Table II, it can be observed that the conventional method employed in [7]–[11] leads to overestimated and unrealistic HFAs and DFA. This is an inherent limitation of the conventional method driven by the assumption that each FR type is fully available at each hour. Although this assumption is valid for the reactive power of

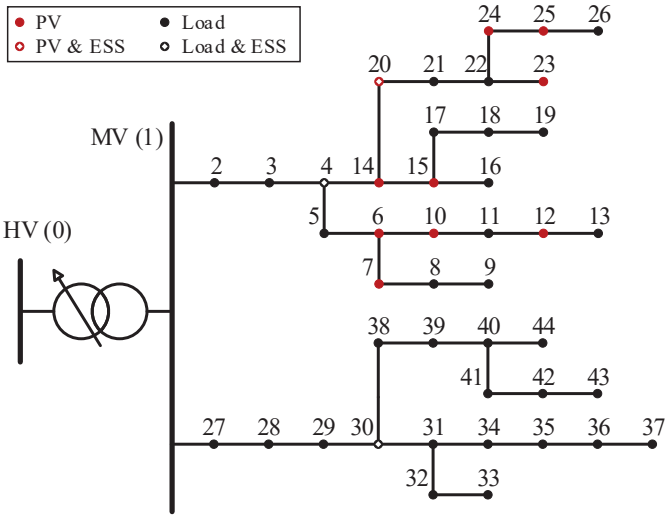

Fig. 3. Topology of the examined MV network.

TABLE I
ESS Characteristics

E_b	$P_{\max}$	η	$SoC_{\min}$	$SoC_{\max}$
500 kWh	250 kW	0.95	10 %	100 %

PV units, it cannot be applied to ESSs since the available active power strongly depends on the state of charge and the operating conditions of the previous/next hour.

On the other hand, the approach presented in [16] leads to more conservative results compared to the proposed method. More specifically, according to Table II, the DFA is reduced by almost 40 % compared to the proposed solution. This can be justified by the fact that contrary to the fixed ESS operation pattern assumed in [16], the ESS operation pattern is indirectly introduced as a control variable in the optimization problem of the proposed method as expressed by (1)-(15). Similar conclusions can be drawn for the HFAs depicted in Fig. 4.

Although no active power based FR is used in the approach presented in [16], the distribution grid can provide active power flexibility, as verified in Figs. 4-5, reaching up to 6.5 % of the daily mean active energy at the TSO-DSO interface. This is justified by the fact that the reactive power used by the FRs affects the network active losses an thus the daily active energy delivered at the TSO-DSO interface. Following a similar rational, the daily reactive energy at the TSO-DSO interface can be modified by only using active power based FRs. This is an important observation highlighting the ability to provide active (reactive) power flexibility even in cases active (reactive) power based FRs are absent.

It is worth mentioning that the daily sum of the HFAs is always smaller than the DFA for all the examined methods. Indicatively, in the proposed method, the daily sum of HFAs is equal to 68.24 MVAh^2 while the corresponding DFA is 706.04 MVAh^2. The main reason behind this deviation lies on the definition of HFA and DFA, where the former uses hourly data while the latter daily data. For example, let assume that the HFA is constant for the whole day forming a rectangle

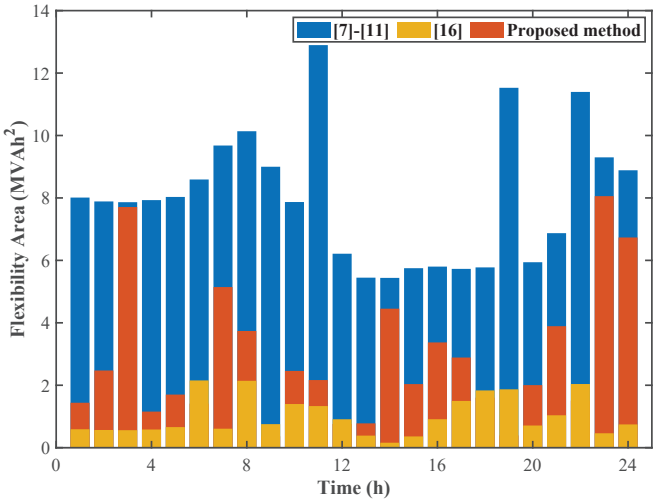

Fig. 4. Hourly flexibility areas (HFAs).

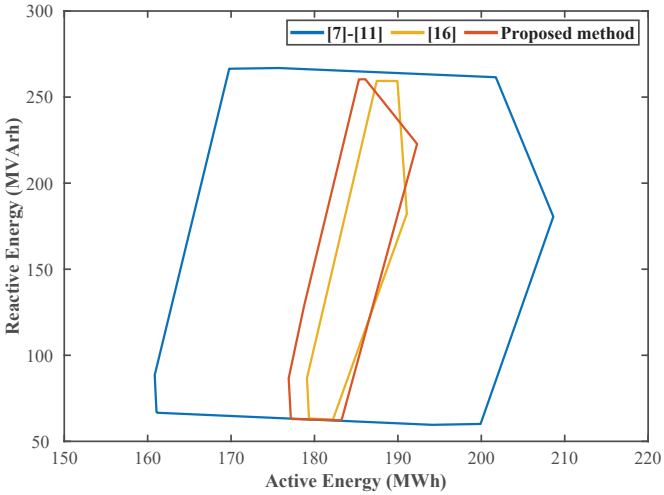

Fig. 5. Daily flexibility area (DFA).

TABLE II
DAILY FLEXIBILITY AREAS (MVAh^2)

	[7]–[11]	[16]	Proposed
Flexibility Area	4228.26	422.41	706.04
Difference (%)	498.87	-40.17	0.00

with edges P and Q. Then, the daily sum of HFA is $24PQ$ and the corresponding DFA is $24P24Q$, where $24P$ and $24Q$ are the cumulative daily flexibility edges.

B. Evaluation of the Second Stage

The outcome of the first stage is the HFAs that are forwarded to the TSO or the Market Operator for the day-ahead planning of the electrical grid. In this paper, the hourly active and reactive power set-points are randomly selected from the HFAs estimated at the first stage and depicted in Fig. 6. It can be seen that the reactive power presents a higher flexibility range compared to the active power, since the installed capacity of PV units exceeds the installed capacity of ESSs. Furthermore, during high generation periods, the reactive power flexibility range is reduced since part of the available reactive power of PV units is used to tackle

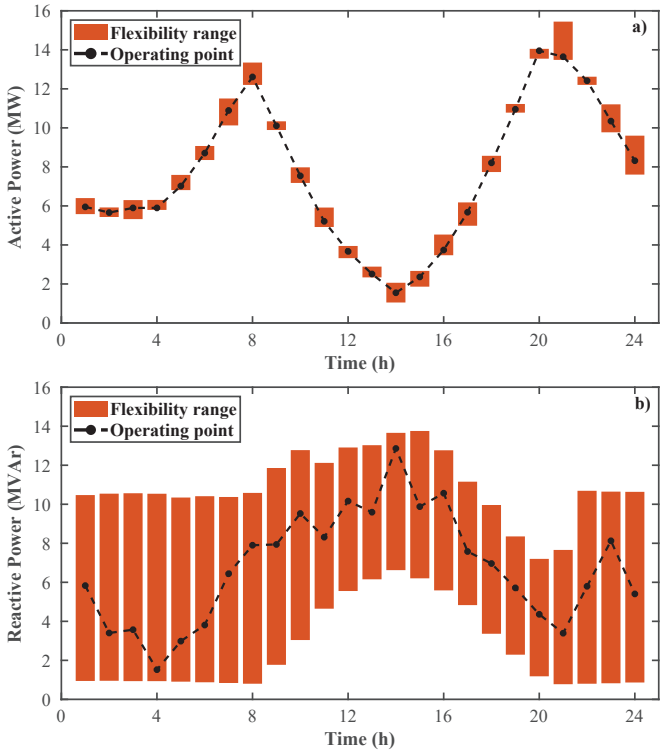

Fig. 6. Daily aggregated power profiles at TSO-DSO interface. a) Active power and b) reactive power. Positive sign indicates downstream power flow, i.e., from HV to MV grid.

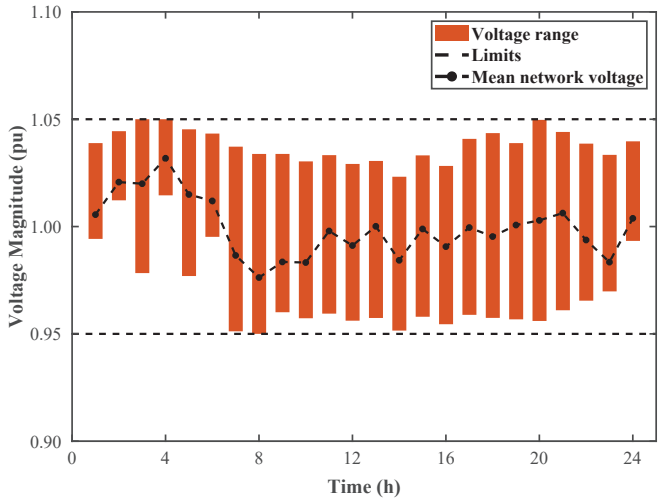

Fig. 7. Daily voltage profile.

overvoltages which usually occur at the most distant nodes of the distribution grid.

The results of the second stage of the proposed methodology are presented in Figs. 7 and 8. More specifically, the hourly range of the network voltages are presented in Fig. 7. It can be observed that the proposed method respects the technical limits posed by the distribution grid, since the network voltages remain within the permissible limits of ± 5 % of the nominal voltage [18]. Furthermore, the hourly overall reactive power profile of PV units and the active power profile of ESSs are presented in Fig. 8. Note that all ESSs present a reduced usage which improves their lifetime.

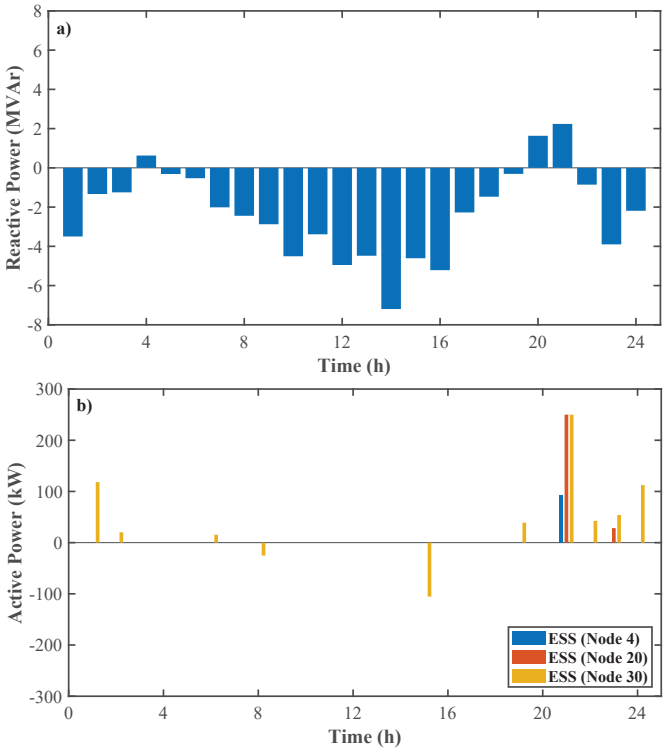

Fig. 8. Daily power profiles of FRs. a) Overall reactive power of PV units and b) ESS active power.

IV. Conclusions and Future Work

In this paper, a two-stage method is proposed for the provision of time-dependent flexibility at the TSO-DSO interface. More specifically, an iterative, multi-period optimization process is applied to the first stage aiming to determine the HFAs that maximize the DFA. The estimated HFAs can be used as input in the day-ahead planning of the electrical grid. The second stage is employed to optimally coordinate the FRs to meet the operating setpoints at the TSO-DSO interface determined by the day-ahead planning. The validity of the proposed method is demonstrated by performing simulations on a MV distribution grid with radial configuration, highlighting its improved performance compared to the current state of the art methods in terms of accurate estimation of flexibility areas.

Future work will be carried out to consider additional control variables, e.g., tap^t, and operating constraints, e.g., equal SoC at the beginning and the end of the day. Furthermore, an additional algorithm will be implemented to ensure that the active and reactive power at the TSO-DSO meets the predefined operating set-points under real-time conditions. Finally, the integration of generation and consumption uncertainty in the optimization problem will be investigated.

Acknowledgment

This research is co-financed by Greece and the European Union (European Social Fund - ESF) through the Operational Programme "Human Resource Development, Education and Lifelong Learning" in the context of the project "Reinforcement of Postdoctoral Researchers - 2nd Cycle" (MIS-5033021), implemented by the State Scholarships Foundation.

Ευρωπαϊκή Ένωση
European Social Fund

Operational Programme
Human Resources Development,
Education and Lifelong Learning
Co-financed by Greece and the European Union

ΕΣΠΑ 2014-2020

References

[1] T. L. Vu and K. Turitsyn, "A framework for robust assessment of power grid stability and resiliency," *IEEE Trans. Autom. Control*, vol. 62, no. 3, pp. 1165–1177, 2017.

[2] S. Riaz and P. Mancarella, "On feasibility and flexibility operating regions of virtual power plants and TSO/DSO interfaces," in *2019 IEEE Milan PowerTech*, 2019, pp. 1–6.

[3] F. L. Müller, J. Szabó, O. Sundström, and J. Lygeros, "Aggregation and disaggregation of energetic flexibility from distributed energy resources," *IEEE Trans. Smart Grid*, vol. 10, no. 2, pp. 1205–1214, 2019.

[4] G. De Zotti, S. A. Pourmousavi, J. M. Morales, H. Madsen, and N. K. Poulsen, "Consumers' flexibility estimation at the TSO level for balancing services," *IEEE Trans. Power Syst.*, vol. 34, no. 3, pp. 1918–1930, 2019.

[5] M. Heleno, R. Soares, J. Sumaili, R. J. Bessa, L. Seca, and M. A. Matos, "Estimation of the flexibility range in the transmission-distribution boundary," in *2015 IEEE Eindhoven PowerTech*, 2015, pp. 1–6.

[6] D. Mayorga Gonzalez, J. Hachenberger, J. Hinker, F. Rewald, U. Häger, C. Rehtanz, and J. Myrzik, "Determination of the time-dependent flexibility of active distribution networks to control their TSO-DSO interconnection power flow," in *2018 Power Syst. Comput. Conf. (PSCC)*, 2018, pp. 1–8.

[7] H. Chen and A. Moser, "Improved flexibility of active distribution grid by remote control of renewable energy sources," in *2017 6th Int. Conf. Clean Elect. Power (ICCEP)*, 2017, pp. 280–284.

[8] F. Capitanescu, "TSO–DSO interaction: Active distribution network power chart for tso ancillary services provision," *Elect. Power Syst. Res.*, vol. 163, pp. 226 – 230, 2018.

[9] N. Savvopoulos and N. Hatziargyriou, "Estimating operational flexibility from active distribution grids," in *2020 17th Int. Conf. European Energy Market (EEM)*, 2020, pp. 1–6.

[10] J. Silva, J. Sumaili, R. J. Bessa, L. Seca, M. A. Matos, V. Miranda, M. Caujolle, B. Goncer, and M. Sebastian-Viana, "Estimating the active and reactive power flexibility area at the TSO-DSO interface," *IEEE Trans. Power Syst.*, vol. 33, no. 5, pp. 4741–4750, 2018.

[11] J. Silva, J. Sumaili, R. J. Bessa, L. Seca, M. Matos, and V. Miranda, "The challenges of estimating the impact of distributed energy resources flexibility on the TSO/DSO boundary node operating points," *Comput. & Oper. Res.*, vol. 96, pp. 294 – 304, 2018.

[12] M. Kalantar-Neyestanaki, F. Sossan, M. Bozorg, and R. Cherkaoui, "Characterizing the reserve provision capability area of active distribution networks: A linear robust optimization method," *IEEE Trans. Smart Grid*, vol. 11, no. 3, pp. 2464–2475, 2020.

[13] D. A. Contreras and K. Rudion, "Improved assessment of the flexibility range of distribution grids using linear optimization," in *2018 Power Syst. Comput. Conf. (PSCC)*, 2018, pp. 1–7.

[14] E. Polymeneas and S. Meliopoulos, "Aggregate modeling of distribution systems for multi-period OPF," in *2016 Power Syst. Comput. Conf. (PSCC)*, 2016, pp. 1–8.

[15] Z. Tan, H. Zhong, Q. Xia, C. Kang, X. S. Wang, and H. Tang, "Estimating the robust P-Q capability of a technical virtual power plant under uncertainties," *IEEE Trans. Power Syst.*, vol. 35, no. 6, pp. 4285–4296, 2020.

[16] D. A. Contreras and K. Rudion, "Time-based aggregation of flexibility at the TSO-DSO interconnection point," in *2019 IEEE Power Energy Soc. General Meeting (PESGM)*, 2019, pp. 1–5.

[17] D. Bertsimas and J. N. Tsitsiklis, *Introduction to linear optimization*. Belmont Massachusetts: Athena Scientific, 1997.

[18] G. C. Kryonidis, C. S. Demoulias, and G. K. Papagiannis, "A new voltage control scheme for active medium-voltage (MV) networks," *Elect. Power Syst. Res.*, vol. 169, pp. 53–64, Apr. 2019.

[19] G. C. Kryonidis, "Hourly generation and consumption data for estimating the flexibility at TSO-DSO interface," 2021. [Online]. Available: https://dx.doi.org/10.21227/bphb-a466

[20] R. E. Rosenthal, *GAMS: A User's Guide*, GAMS Development Corporation, Washington, DC, USA, 2016.